Supporting Information

Wu et al. 10.1073/pnas.0904792106

SI Text

Synthesis of Oleic Acid-decorated β-NaY$_{0.78}$F$_4$:Yb$_{0.2}$ Er$_{0.02}$ Nanoparticles. All of the syntheses were performed using standard oxygen-free conditions except where noted. All chemicals were used without further purification. Rare earth oxides (Yb_2O_3, Er_2O_3), oleic acid (OA, 90%), oleylamine (OM, >70%), 1-octadecene (ODE >90%), trifluoroacetic acid (99%), CF_3COONa, $Y(CF_3COO)_3$, citric acid, absolute ethanol, and hexane were purchased from Sigma-Aldrich. $Yb(CF_3COO)_3$ and $Er(CF_3COO)_3$ were prepared by the methods reported (1).

The monodispersed oleic acid decorated β- NaY$_{0.78}$ F$_4$: Yb$_{0.2}$ Er$_{0.02}$ nanoparticles were prepared by a 2-step reaction that is similar to the procedure reported by Mai et al. (2). The α-NaY$_{0.78}$F$_4$:Yb$_{0.2}$ Er$_{0.02}$ nanocrystals were synthesized in the first step. 1 mmol CF_3COONa, 0.78 mmol $Y(CF_3COO)_3$, 0.2 mmol $Yb(CF_3COO)_3$ and 0.02 mmol $Er(CF_3COO)_3$ were added to a mixture of 10 mmol OA, 10 mmol OM, and 20 mmol ODE in a 50-mL, 3-necked flask followed by a 30-min vacuum to remove water and oxygen at 100 °C. Then, the reaction mixture was heated to 290 °C and reacted for 45 min under N_2 flow. The reaction was quenched by removing the heat followed by adding in excess absolute ethanol. The resultant turbid solution was then centrifuged to yield white precipitates. Such precipitates was then washed with ethanol 4 times and dried in the vacuum oven at 70 °C overnight to afford the α-NaY$_{0.78}$F$_4$:Yb$_{0.2}$ Er$_{0.02}$ nanocrystals. The β-NaY$_{0.78}$F$_4$:Yb$_{0.2}$ Er$_{0.02}$ nanocrystals were prepared using such α-phase nanoparticles as precursors at the second step. One mmol CF_3COONa and 1.3 mmol α-NaY$_{0.78}$F$_4$:Yb$_{0.2}$ Er$_{0.02}$ were added to a mixture of 20 mmol OA and 20 mmol ODE in a 50-mL, 3-necked flask followed by a 30-min vacuum to remove water and oxygen at 100 °C. Then, the reaction mixture was heated to 330 °C and reacted for 15 min under N_2 flow. The reaction was quenched by removing the heat followed by adding in excess absolute ethanol. The resultant turbid solution was then centrifuged to yield white precipitates. Such precipitates was then washed with ethanol 4 times and dried in the vacuum oven at 70 °C overnight. The afforded β-NaY$_{0.78}$F$_4$:Yb$_{0.2}$Er$_{0.02}$ nanocrystals can dissolve in hexane, cyclohexane, and other nonpolar solvents.

Synthesis of Citric Acid and Amphiphilic Polymer-decorated β-NaY$_{0.78}$F$_4$:Yb$_{0.2}$ Er$_{0.02}$ Nanoparticles. The synthesis scheme of both water-soluble UCNPs is shown in Fig. S4*A*. To obtain citric acid coated UCNPs (CA-UCNPs), 10 mg oleic acid decorated β-NaY$_{0.78}$F$_4$:Yb$_{0.2}$ Er$_{0.02}$ nanoparticles (OA-UCNPs) was stirred suspension with 0.2 M citric acid for 16 h. The pH of the reaction mixture was adjusted to 10 with 0.1 M NaOH, and the resultant solution was spin-dialyzed against purified water (30-kDa molecular weight cutoff, Amicon) followed by filtration through a 0.2-μm filter.

Alternatively, the amphiphilic polymer decorated UCNPs (AP-UCNPs) were achieved using octylamine-modified poly-(acrylic acid) (MW = ≈3000 Da, OPA) (3). Briefly, 1.5 mg OA-UCNPs in 1 mL chloroform stirred with 30 mg OPA in 4 mL choroform for 15 min at room temperature followed by removal of all of the solvents using rotavapor. The afforded residue can readily dissolve in slightly basic water (pH = 9). The resultant solution was spin-dialyzed against purified water or buffer (30-kDa molecular weight cutoff, Amicon) followed by filtration through a 0.2-μm filter to remove excess polymers.

The afforded CA-UCNPs and AP-UCNPs in water appear to be well-dispersed as found in the Dynamic light scatting experiments (zetasizer, nano-zs, Malvern). (see Fig. S4*B*)

1. Roberts JE (1961) Lanthanum and neodymium salts of trifluoroacetic acid. *J Am Chem Soc* 83:1087–1088.
2. Mai HX, Zhang YW, Sun LD, Yan CH (2007) Highly efficient multicolor up-conversion emissions and their mechanisms of monodisperse NaYF$_4$:Yb,Er core and core/shell-structured nanocrystals. *J Phys Chem C* 111:13721–13729.
3. Zhou M, et al. (2007) Peptide-labeled quantum dots for imaging GPCRs in whole cells and as single molecules. *Bioconjugate Chem* 18:323–332.

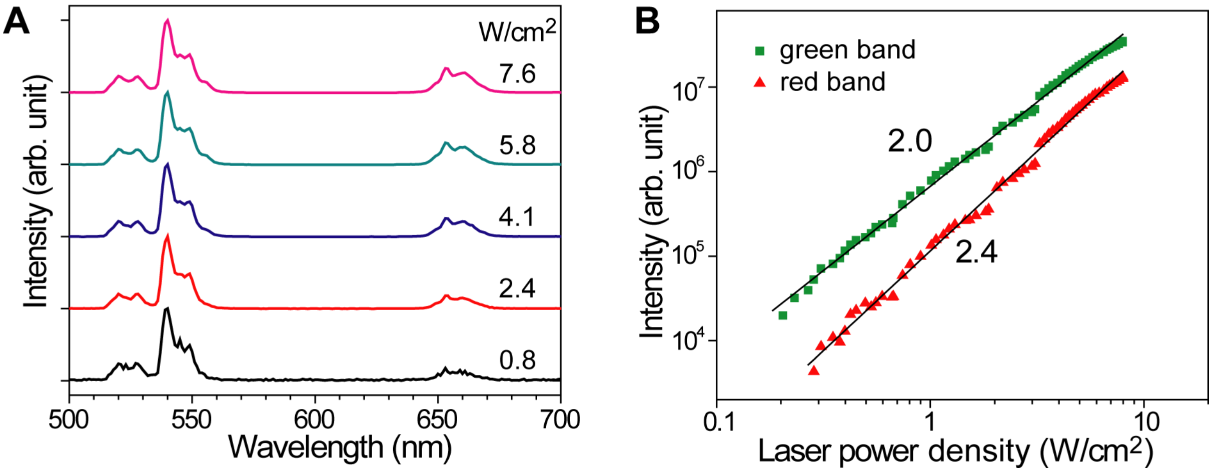

Fig. S1. Upconverted luminescent spectra of the UCNPs in solution and their dependence on power density. (*A*) A sequence of spectra as a function of laser power density, when the UCNP solution (0.01 wt% in hexane) was excited by a 980-nm CW diode laser. All of the spectra were normalized to the peak at 540 nm and are offset for comparison. The intensity of red upconverted emission (640–680 nm) increases faster than that of the green emission (510–560 nm). (*B*) Intensities of the green and red emission were plotted as a function of laser power density. The double-logarithmic plots were fitted linearly, yielding a slope of 2.0 for the green emission and a slope of 2.4 for the red emission. The slopes suggest that the green emission is dominated by a 2-photon upconversion process and the red emission is a result of mixed multiphoton ($n = 2$ and $n > 2$) upconversion processes.

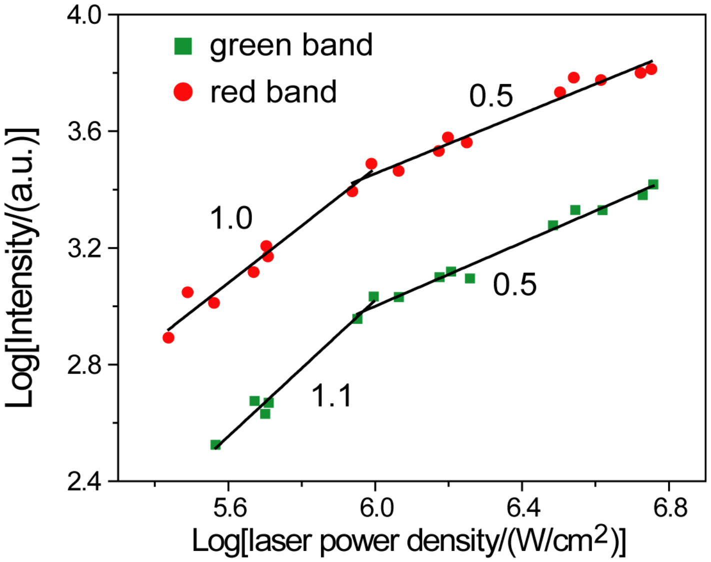

Fig. S2. Power dependence of the green and red upconverted luminescence of a single UCNP. The green and red emission bands were separated from the upconverted luminescence through two additional filters, D560/60M and HQ665/45M (Chroma), respectively. The figure is plotted in a double-logarithmic format. Because the 980-nm CW laser was tightly focused, the power density is much higher than that used to excite the ensembles. The high power density results in saturation of the upconversion processes, as shown by the reduction in fitted-line slopes (as labeled). We note that the intensity of the red emission is actually higher than that of the green emission, because of the faster intensity rise for the red light when the laser power increases (see Fig. S1).

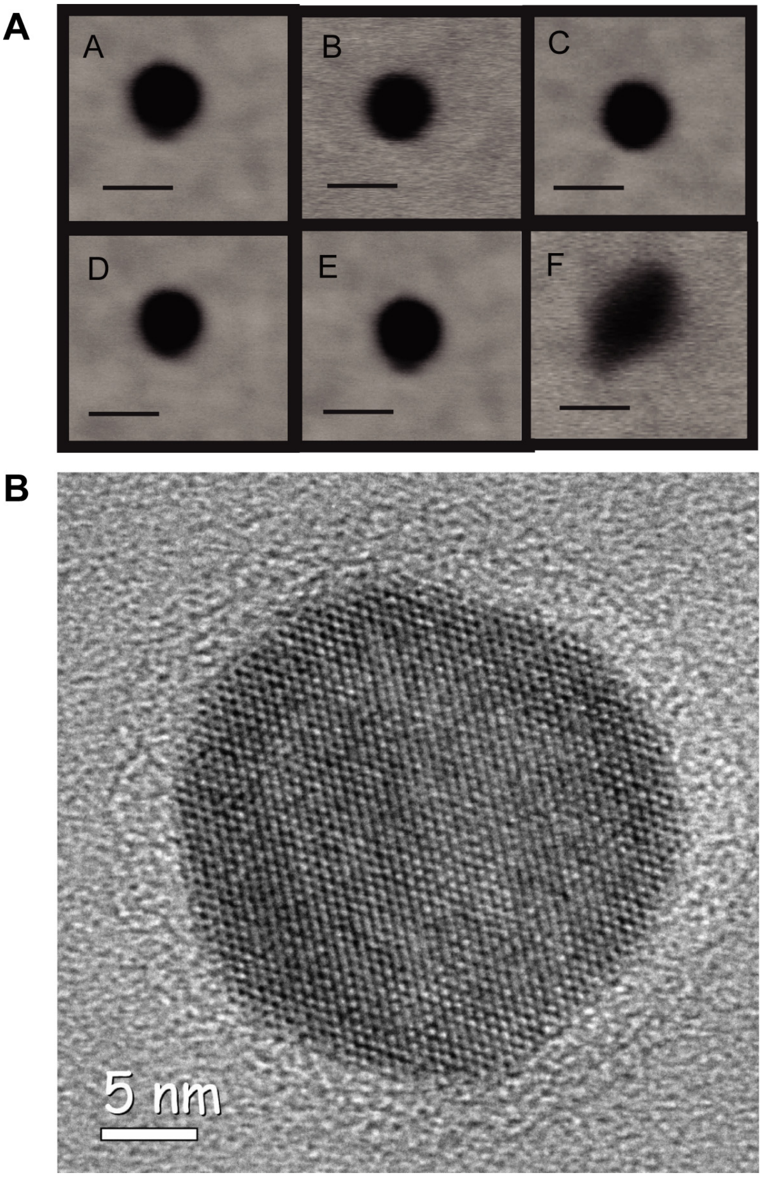

Fig. S3. TM-SEM and HR-TEM images of individual UCNPs. (*A*) TM-SEM images of individual UCNPs (A–E) and impurity (F) shown in the inset of Fig. 2*A*. (Scale bar, 30 nm.) Their shape and size, together with X-ray EDS analysis, are summarized in Table S1. (*B*) HR-TEM image of a single UCNP.

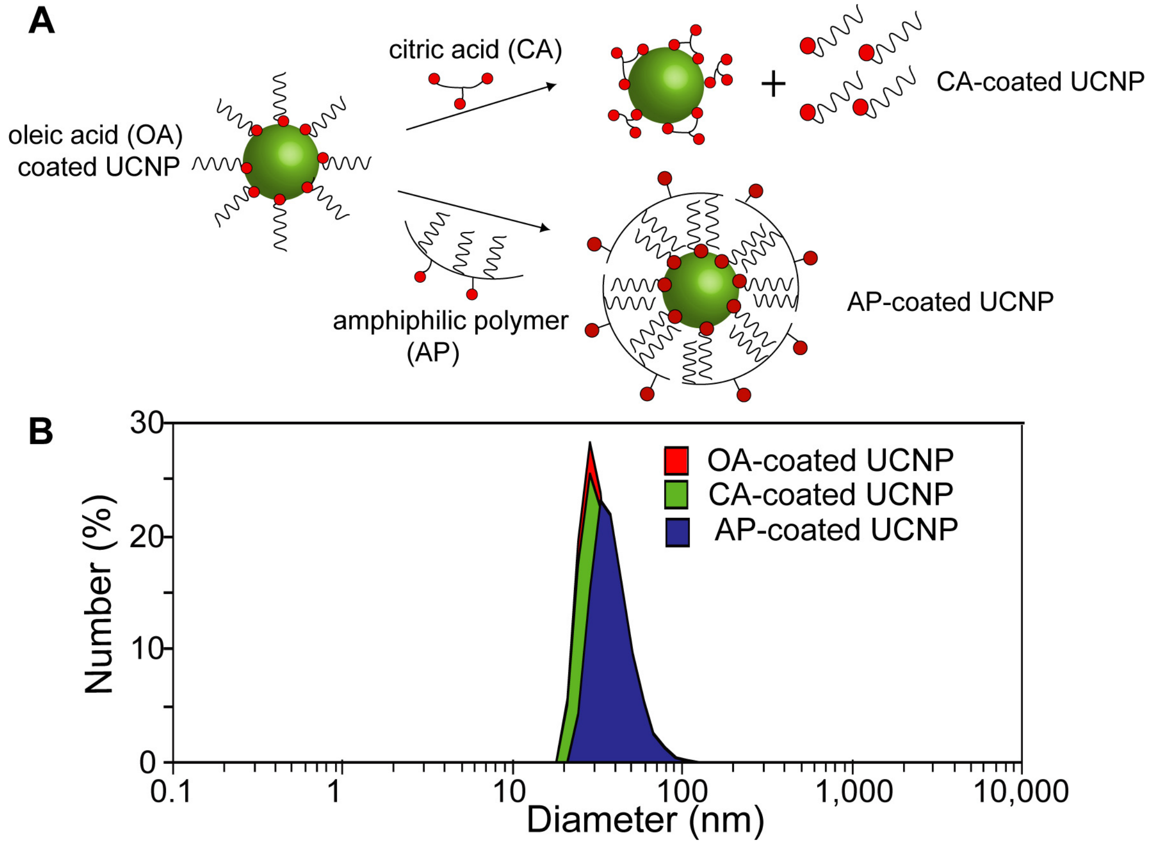

Fig. S4. Synthesis of amphiphilic polymer-coated UCNPs and citric acid-coated UCNPs. (*A*) Schematics showing that the amphiphlic polymer-coated UCNPs were prepared by coating the oleic acid-coated UCNPs with amphiphilic polymers; while the citric acid coated UCNPs were made by exchange of surface oleic acid with citric acid. Both methods result in water-soluble UCNPs, as opposed to the hydrophobic oleic acid-coated UCNPs. (*B*) Dynamic light scattering data showing the particle sizes of well-dispersed UCNPs in solution. The polymer-coated UCNPs in water have slightly larger particle size (40 nm), while the citric acid-coated UCNPs (29 nm) have similar particle size as the oleic acid-coated UCNPs (31 nm).

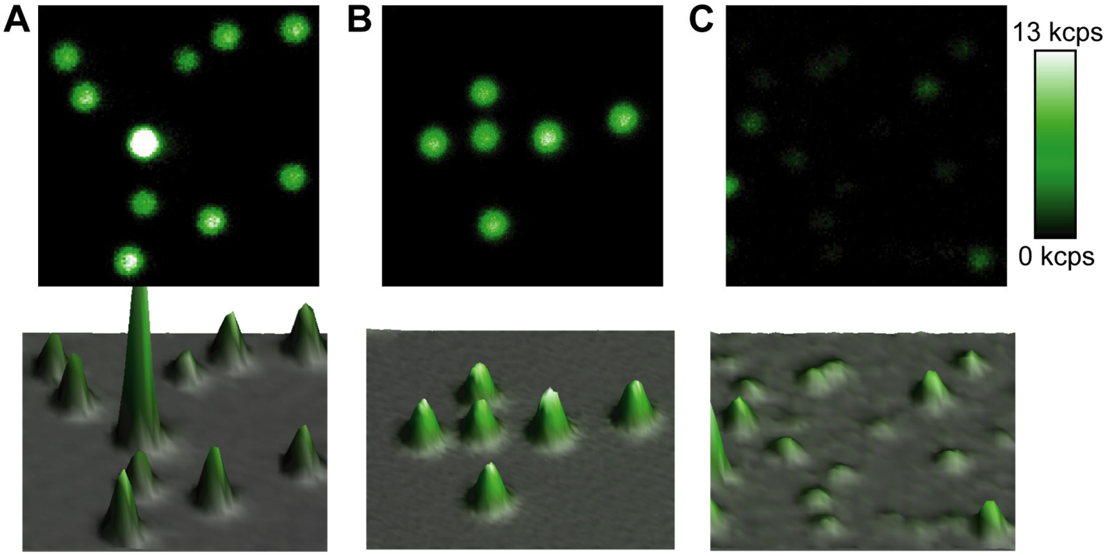

Fig. S5. Confocal upconverted luminescent images of individual UCNPs with different surface functionalizations. (*A*) Oleic acid-coated UCNPs. (*B*) Amphiphilic polymer-coated UCNPs. (*C*) Citric acid-coated UCNPs. These confocal images were measured with the same laser power (≈10 mW or ≈5 × 10^6 W/cm^2). Image size is 10 × 10 μm.

Table S1. The list of the identities of the individual UCNPs and nearby impurity (F) in Fig. S3

	Shape	Diameter (nm)	Y: Yb: Er (at%)*
A	Sphere	27.8	78.0: 19.8: 2.2
B	Sphere	27.9	79.3: 18.3: 2.4
C	Sphere	28.7	79.5: 18.5: 2.0
D	Sphere	28.6	78.6: 19.4: 2.0
E	Sphere	28.8	79.1: 18.9: 2.0
F	Irregular Shape	55.4	−: −: −

*Y:Yb:Er elemental ratios were obtained using their respective K_α, L_α and L_α lines from EDS spectra acquired under TEM at 200 kV (values have an error of about 0.7 at%).